JOURNAL OF AGRICULTURAL AND FOOD CHEMISTRY

Article

pubs.acs.org/JAFC

Role of the N-Terminal Amphiphilic Region of Ovalbumin during Heat-Induced Aggregation and Gelation

Yuki Kawachi,[†] Rina Kameyama,[†] Akihiro Handa,[§] Nobuyuki Takahashi,[#] and Naoki Tanaka*[,†]

[†]Department of Bio-molecular Engineering, Kyoto Institute of Technology, Matsugasaki, Sakyo, Kyoto 606-8585, Japan

[§]R&D Division, Institute of Technology, Kewpie Corporation, 5-13-1 Sumiyoshi, Fuchu, Tokyo 183-0034, Japan

[#]Graduate School of Agriculture, Kyoto University, Uji, Kyoto 611-0011, Japan

Supporting Information

ABSTRACT: Ovalbumin (OVA), a major globular protein in egg white, forms semiflexible fibrillar aggregates during heat-induced gelation. The N-terminal amphiphilic region (pN_{1-22}) of OVA is removed after treatment with pepsin at pH 4 to leave a large OVA fragment (pOVA). The conformation and thermal stability of pOVA and OVA are similar, but the rheological strength of the heat-induced gel of pOVA is much lower compared to that of OVA. The aggregation rate of pOVA, which forms spherical aggregates, was lower than that of OVA. These results suggest that the N-terminal amphiphilic region of OVA facilitates the α-to-β conformational transition, which triggers OVA fibril formation. Heat treatment of OVA in the presence of pN_{1-22} consistently resulted in the formation of straight fibrils. The strength of OVA and collagen gels was increased when prepared in the presence of pN_{1-22}, suggesting that pN_{1-22} may be used to control the properties of protein gels.

KEYWORDS: *ovalbumin, aggregation, gelation, amphiphilic region, amyloid fibril*

INTRODUCTION

Ovalbumin (OVA), a major globular protein in egg white, is a glycoprotein composed of 385 amino acid residues with a molecular mass of 45 kDa and an isoelectric point of 4.5. Its overall crystal structure contains ca. 35% α-helix and ca. 45% β-sheet (Figure 1).[1,2] The heat-induced aggregation and gelation of OVA have been extensively studied due to the importance of OVA in the food industry.[3] Upon heating, OVA undergoes a two-state unfolding process with a midpoint temperature of 76 °C at neutral pH[4] or 57 °C at pH 2.2.[5] However, a significant degree of secondary structure is retained in the heat-induced unfolded state.[4,6] Although the heat-induced unfolding of OVA is nearly reversible in the absence of salt at neutral pH, it is completely irreversible in the presence of salt due to the formation the fibrillar aggregates.[4,7−15] The morphology of OVA fibrils is dependent on various factors such as salt concentration, surface charge, and reduction of disulfide bonds.[11,13−15] A recent study indicated that several types of fibrils with clear structural and physical differences were formed during the heat treatment at low pH and high temperature.[15]

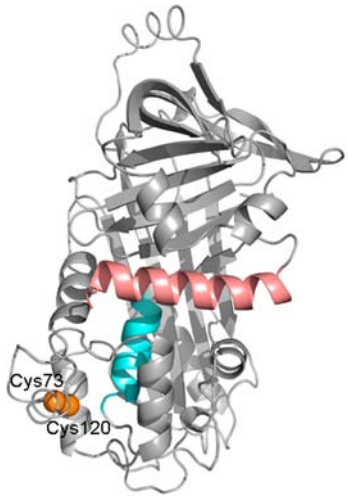

Figure 1. Schematic illustration of a 3D ribbon model of OVA (PDB code, 1OVA)[2] drawn with Pymol. The regions include the residues from 1 to 22 of helix A and the residues from 32 to 43 of helix B are colored red and cyan, respectively. Cys73 and Cys120 are shown as orange spheres.

The mechanism of formation of amyloid fibrils, the fibrillar aggregates related to various human diseases such as Alzheimer's and Parkinson's diseases, has been extensively studied.[16−19] The aggregation of OVA is amyloid-like owing to the formation of a β-conformation as monitored by CD spectroscopy as well as an increase in thioflavin T fluorescence.[8,9,20] In a previous study, we analyzed the mechanism of formation of OVA fibrillar aggregates by using synthetic peptide fragments and by site-directed mutagenesis.[14] The hydrophobic region composed of residues 32−43 of helix B (IAIMSALAMVYL; cyan colored in Figure 1) was identified as the core region that induces the α-to-β conformational transition and triggers the formation of fibrillar aggregates. Heat treatment of OVA at high protein concentration results in gelation due to the formation of a network of fibrillar aggregates.[21,22] The properties of the heat-induced gel are strongly dependent on pH, with a turbid and hard gel formed

Received: June 5, 2013
Revised: July 26, 2013
Accepted: August 4, 2013
Published: August 5, 2013

close to the isoelectric point of OVA. In contrast, a transparent gel is formed at pH 2 and 7 in the absence of salt, or a turbid and hard gel is formed at higher salt concentration at the same pH.[21,23−26]

Interestingly, the properties of the heat-induced gel are affected by the truncation of the N-terminal residues from 1 to 22 of OVA.[27−29] The pepsin hydrolysis of OVA at pH 4 cleaves a single peptide bond between His22 and Ala23 to remove the N-terminal amphiphilic peptide of helix A (acetyl-GSIGAA-SMEFCFDVFKELKVHH (pN_{1-22}); red colored in Figure 1) from a large OVA fragment called pOVA. The physicochemical properties such as intrinsic viscosity and secondary structure shown by the CD spectrum of pOVA were similar to those of OVA. However, heat treatment of pOVA resulted in the formation of a transparent gel with lower strength than the OVA gel prepared under the same conditions.

OVA is the major secretory protein from hen oviduct, and its secretion signal sequence is located within residues 22−41.[30−32] This is unusual given that the N-terminal signal sequences of many secretory proteins are proteolytically removed before secretion. Residues 9−21 of helix A (EFCFDVFKELKVH) are important for OVA translocation through the membrane. Indeed, an engineered form of OVA lacking these residues is sequestered in the endoplasmic reticulum and is strongly associated with the membrane.[30] Therefore, the amphiphilic property of helix A may play a role in dissociating the newly synthesized OVA from the membrane to facilitate secretion.

A thorough analysis of the aggregation and gelation of pOVA is important for understanding the mechanism of the heat-induced gelation of OVA. However, to date, a detailed study of the heat-induced aggregation of pOVA has not been reported. Here, we have investigated the role of the N-terminal amphiphilic region of OVA by analyzing the aggregation and gelation of OVA and pOVA using electron microscopy as well as spectroscopic and rheological measurements. Furthermore, the effects of pN_{1-22} on the aggregation and gelation of OVA were studied. Our results indicate that the N-terminal amphiphilic region plays a significant role in the heat-induced aggregation of OVA, and pN_{1-22} could potentially be used to control the properties of protein gels in the food industry.

MATERIALS AND METHODS

Materials. OVA (98% pure, product no. A5503) and pepsin from porcine stomach were purchased from Sigma-Aldrich (St. Louis, MO, USA) and Worthington Biochemicals Co. (Lakewood, NJ, USA), respectively. pOVA was prepared by treating OVA with pepsin at pH 4.0 as reported previously.[27] Briefly, OVA was incubated at 25 °C with pepsin (1/50 w/w ratio of pepsin/OVA) in 100 mM sodium acetate (pH 4.0) for 12 h, before the solution was neutralized (pH 7.0) to terminate the reaction. Pepsin was then removed by passing the solution through DEAE. The relatively small pN_{1-22} fragment was subsequently eliminated by dialysis. The heat-induced gels were prepared by incubation of a protein solution in 100 mM potassium phosphate (pH 2.2) at 65 °C for 1 h. The acid-soluble type I collagen I from porcine tendon (Cellmatrix Type I-A) was purchased from Nitta gelatin (Osaka, Japan). Collagen fibrils were reconstituted according to a modified protocol supplied by the manufacturer. Specifically, eight parts of the collagen I solution (3.0 mg/mL, pH 3.0) were mixed with two parts of 100 mM potassium phosphate (pH 7.5). All peptides used in this study were synthesized and purified by GenScript (Piscataway, NJ, USA).

Turbidity Measurement. Protein solutions were diluted in 100 mM phosphate buffer (pH 2.2) that had been preheated to 65 °C. Dilution was performed in an optical cell placed in a spectrophotometer so that the final protein concentration was 0.26 mg/mL. After the cuvettes had been capped, the kinetics of aggregation at 65 °C were monitored by measuring the change in the turbidity of the solution at 320 nm.

Gel Permeation Chromatography (GPC) Assay. OVA (0.26 mg/mL) in 100 mM potassium phosphate (pH 2.2) was incubated at 65 °C for various periods of time and then cooled to room temperature. The solution was then subjected to centrifugation at 15000*g* for 5 min to remove large aggregates. Monomers and small aggregates in the supernatants were separated by gel filtration chromatography using a Superdex 200 column (GE Healthcare, Piscataway, NJ, USA). The concentration of OVA monomers in the supernatant was determined from the intensity of the monomer peak in the chromatogram as reported previously.[33] The self-association of pN_{1-22} was monitored by gel filtration chromatography using a Superdex Peptide column (GE Healthcare).

Circular Dichroism (CD) Spectroscopy. The secondary structure of OVA was monitored by CD spectroscopic measurements using a Jasco J-720 instrument (Tokyo, Japan). An optical quartz cell with a 1 mm path length was used. Far-UV spectra were obtained at 25 °C using a scan speed of 20 nm/min.

Transmission Electron Microscopy (TEM). TEM images of OVA aggregates and amyloid fibrils of peptides were acquired with a JEM-1200EX II instrument (JEOL, Tokyo, Japan) using an acceleration voltage of 85 keV. One millimolar potassium phosphate (pH 2.2) was used as the solvent. Heat-induced aggregates were obtained by heat treatment of 1.0 mg/mL protein or peptide solution at pH 2.2 at 65 °C. The samples were negatively stained with 1.5−2.0% phosphotungstate adjusted to pH 7.5 using sodium hydroxide.

Rheology. Rheological experiments were conducted on an AR-1000 rheometer (TA Instruments, Leatherhead, UK) at 25 °C. Measurements were performed using a 2° cone geometry (diameter = 40 mm) with a solvent trap. All experiments were conducted in oscillatory mode with a strain amplitude of 0.5%, which is in the linear viscoelastic regime.

FTIR Spectroscopy. FTIR spectra were recorded using a Spectrum GX FT-IR (PerkinElmer Inc., Waltham, MA, USA). Spectral resolution was 2 cm^{-1}, and the spectra of 64 scans were averaged. The OVA and pOVA were dissolved in D_2O, and the pD was adjusted to 2.2. The solution was heat-treated at 65 °C for 1 h, and the precipitates were washed twice with D_2O. The spectra of protein and peptide samples dried on a CaF_2 window were then measured.

DSC. Calorimetric measurements were performed using a Nano-DSC II model 6100 calorimeter (Calorimetry Science Co., Provo, UT, USA). All experiments were carried out at a scan rate of 1.0 °C/min and protein concentrations of 1.0 mg/mL in 100 mM potassium phosphate (pH 7.5 and 2.2). Data analysis (baseline subtraction and concentration normalization) was performed using software from Calorimetry Science.

RESULTS AND DISCUSSION

Heat-Induced Gelation and Aggregation of OVA and pOVA. Previous studies reported that the conformation of pOVA is similar to that of OVA.[27,28] We confirmed that the secondary structures of pOVA at pH 2.2 and 7.5 are similar to those of OVA based on far-UV CD spectroscopy (Supporting Information, Figure S1). In addition, the thermal transition temperatures of pOVA monitored by DSC were almost the same as those of OVA (Supporting Information, Figure S2; ca.77 °C at pH 7.5 and ca. 55 °C at pH 2.0). Thus, the native conformations of pOVA and OVA display similar thermal stabilities, indicating that the N-terminal amphiphilic region of OVA does not significantly contribute to the stabilization of the remainder of the protein.

Previous studies reported that the strength of the heat-induced gel of pOVA was lower than that of an equivalent gel formed from OVA.[27,28] To confirm the different strengths of these two types of gel, the storage modulus (G') and loss

dx.doi.org/10.1021/jf402456v | J. Agric. Food Chem. 2013, 61, 8668−8675

modulus (G'') were obtained by rheological measurements. In the heat-denatured state of OVA at neutral pH, thiol−disulfide exchanges of the single disulfide bond between Cys_{73} and Cys_{120} (orange spheres in Figure 1) and the other four free cysteines have been shown to occur.[4] To avoid the thiol−disulfide exchanges and simplify analysis of the results, the aggregation and gelation processes of OVA and pOVA were studied under acidic conditions. Heat-induced gels were prepared by incubation of a 2 wt % protein solution in 100 mM potassium phosphate (pH 2.2) at 65 °C for 1 h. It is clear from Figure 2 that the OVA gel displays a much higher G' value

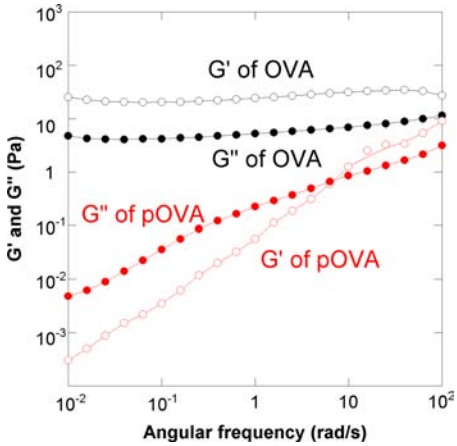

Figure 2. Angular frequency dependence of G' and G'' of OVA gel (black curves) and pOVA gel (red curves): open circles, G'; solid circles, G''. The protein gels were prepared by incubation of a 2 wt % protein solution in 100 mM phosphate (pH 2.2) at 65 °C for 1 h.

than G'' value, indicating it possesses a typical elastic gel network structure. In contrast, the pOVA gel (red plot in Figure 2) shows that G' and G'' are dependent on frequency and have a higher G'' value than G' value in the low angular frequency region, indicating the absence of a gel-like network. Indeed, the G' value of the OVA gel is much higher than that of the pOVA gel at all angular frequencies. These results indicate that the strength of the pOVA gel is much lower than that of the OVA gel as reported previously.[27,28]

Next, we analyzed the likely mechanism of gel formation for OVA and pOVA by studying their respective aggregation. The progress of heat-induced aggregation was monitored by changes in monomer concentration in the protein solution as estimated from the GPC chromatogram.[33] As shown in Figure 3a, the monomer concentrations of pOVA and OVA decreased at the same rate, indicating that monomers of pOVA and OVA display the same heat-induced unfolding rate. The major fraction of the monomers was unfolded and irreversibly aggregated within 3 min after starting the heat treatment. Heat-induced aggregations of OVA and pOVA were also monitored by measuring the turbidity of the solution during the aggregation process. As shown in the inset of Figure 3b, the aggregation rates of OVA and pOVA were similar during the first 3 min of aggregation. On the other hand, the turbidity of pOVA increased to a lesser extent compared with that of OVA in the later stage of aggregation (Figure 3b), in which small aggregates may associate to increase the size. The lower aggregation rate for pOVA may be because the interaction between the pOVA aggregates is lower than that of OVA aggregates.

The structures of heat-induced aggregates of OVA and pOVA were also monitored by TEM. Heat treatment of OVA solution resulted in the formation of semiflexible fibrils (Figure 4a) as reported previously. However, spherical aggregates (Figure 4b) were detected upon heat-induced denaturation of pOVA. The secondary structures of the OVA and pOVA aggregates were analyzed by FTIR spectroscopy. As shown in Figure 5, the profile of the amide I band of the OVA aggregate displayed a maximum at 1625 cm^{-1}, which was not observed in that of intact OVA. This observation indicates that the β-sheet content of the protein is increased upon fibril formation. In contrast, the intensity of the maximum at 1625 cm^{-1} was reduced in the amide I of the pOVA aggregates, suggesting that the β-sheet content of pOVA aggregates is lower than that of OVA aggregates. Thus, reduced formation of semiflexible fibrils in pOVA appears to be due to the lower frequency of the α-to-β conformational transition of the N-terminal amphiphilic region.

Fibril Formation of pN_{1-22} and Its Effect on the Heat-Induced Aggregation of Proteins. Next, we aimed to confirm the role of the N-terminal amphiphilic region of OVA

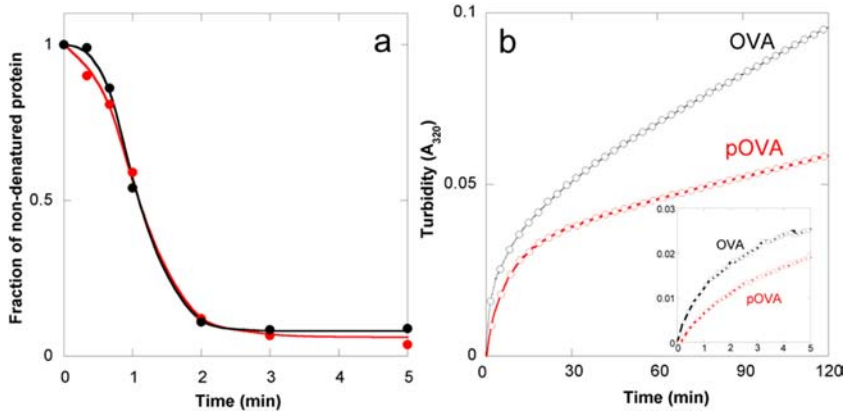

Figure 3. Kinetics of aggregation of OVA and pOVA. (a) The monomer concentration of pOVA and OVA decreased with aggregation. The relative change of monomer concentration was estimated from the monomer peak of GPC analysis of heat-treated OVA solution: black solid circles, OVA; red solid circles, pOVA. (b) The turbidity increased with aggregation at 65 °C: white open circles, OVA; red open circles, pOVA. (Inset) Early stage of aggregation. OVA solution was diluted in 100 mM phosphate buffer (pH 2.2) preheated to 65 °C. The final protein concentration was 0.26 mg/mL.

dx.doi.org/10.1021/jf402456v | J. Agric. Food Chem. 2013, 61, 8668−8675

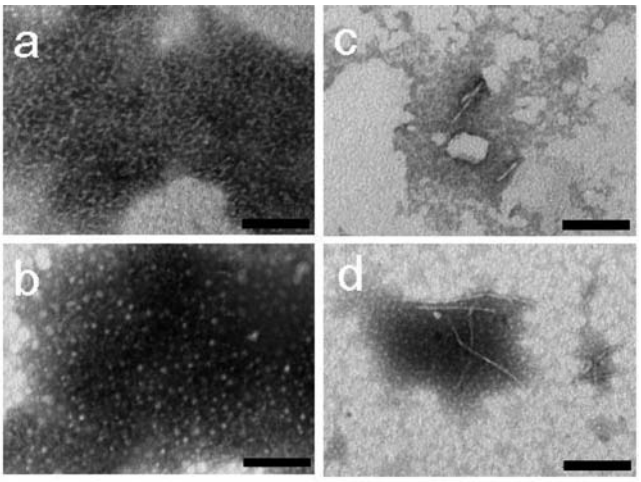

Figure 4. TEM images of heat-induced aggregates of OVA, pOVA, and pN_{1-22}: (a) semiflexible fibrillar aggregates of OVA; (b) particle aggregates of pOVA; (c) fibrillar aggregates of pN_{1-22}. (d) Straight fibrillar aggregates formed in the mixed solution of OVA and pN_{1-22} (molar ratio of OVA/pN_{1-22} = 1:10). Scale bar = 200 nm.

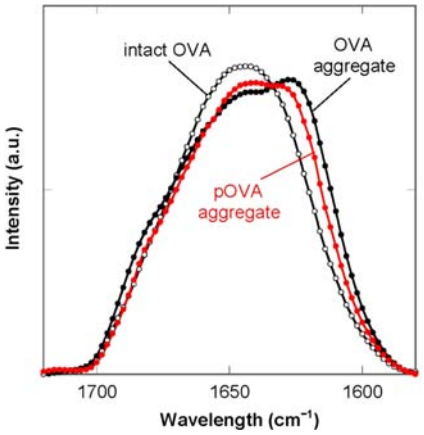

Figure 5. Amide I band of FTIR spectroscopy of OVA and pOVA. The spectra of heat-induced aggregates obtained from OVA and pOVA were compared with that of the spectrum of the intact OVA.

in the formation of the fibrillar aggregates. We therefore studied the effect of pN_{1-22} on the heat-induced aggregation of OVA. pN_{1-22} is soluble in aqueous solution, and the absence of self-association at room temperature was confirmed by GPC. The region corresponding to the sequence of pN_{1-22} is known to adopt an α-helical conformation in the native structure of OVA (Figure 1). Figure 6 shows the far-UV CD spectrum of pN_{1-22} in aqueous solution. The profile of this spectrum with a negative peak at 213 nm indicates that the secondary structure of pN_{1-22} is rich in β-sheet, and the α-helical content was calculated to be only 5% on the basis of the molar value at 208 nm.[34] Therefore, the conformation of pN_{1-22} in solution is significantly different from that in the native structure of OVA.

The effect of heat treatment on the self-association of pN_{1-22} at pH 2.2 was monitored by the turbidity measurement method. As shown in Figure 7, heat treatment of 1.0 mg/mL pN_{1-22} at 65 °C induces an increase in the turbidity with the sigmoidal profile having a lag time of ca. 8 min. TEM analysis showed that a few short fibrils were formed (Figure 4c), whereas the morphology of most of the aggregate was random.

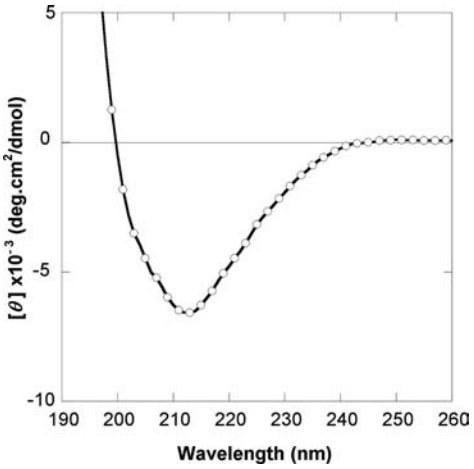

Figure 6. Far-UV CD spectrum of 1.08 mM pN_{1-22} in 100 mM potassium phosphate (pH 2.2) monitored at 25 °C.

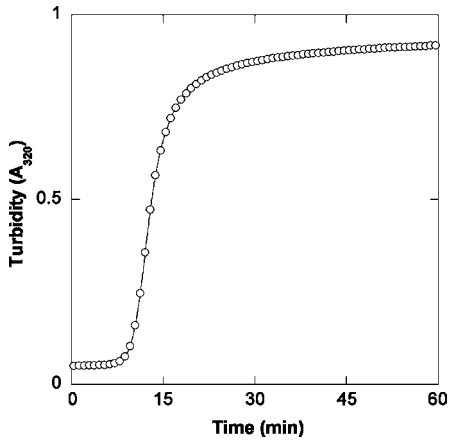

Figure 7. Changes in the turbidity of the solution with the aggregation of 1.0 mg/mL pN_{1-22} in 100 mM sodium phosphate (pH 2.2) at 65 °C.

These results suggest that pN_{1-22} itself has the potential to form amyloid-type aggregates.

The heat-induced aggregation of OVA at pH 2.2 was monitored in the presence of various concentrations of pN_{1-22} by the turbidity measurement method at 65 °C. As shown in Figure 8a, the heat-induced turbidity increase of the OVA solution was accelerated in the presence of pN_{1-22}, indicating that this peptide facilitates the heat-induced aggregation of OVA. Because the turbidity changes seen in this figure are not sigmoidal, the increase in aggregation is not due to the self-association of pN_{1-22}. The effect of pN_{1-22} on the morphology of the OVA aggregates was also studied by TEM measurements. As shown in Figure 4d, straight fibrils, which were distinct from the semiflexible fibrils of OVA, were formed when OVA was co-incubated with pN_{1-22}. These fibrils were much longer than those formed by pN_{1-22} on its own, suggesting that they are distinct from the fibrils of pN_{1-22}. pN_{1-22} may bind with heat-denatured OVA to form straight fibrils composed of OVA and pN_{1-22}.

In a previous study, we reported that the hexapeptide IAIMSA, a soluble peptide fragment corresponding to residues 32−37 of OVA, changes the morphology of the heat-induced aggregates of OVA.[14] IAIMSA corresponds to the N-terminal sequence of helix B (cyan colored in Figure 1), which is

dx.doi.org/10.1021/jf402456v | J. Agric. Food Chem. 2013, 61, 8668−8675

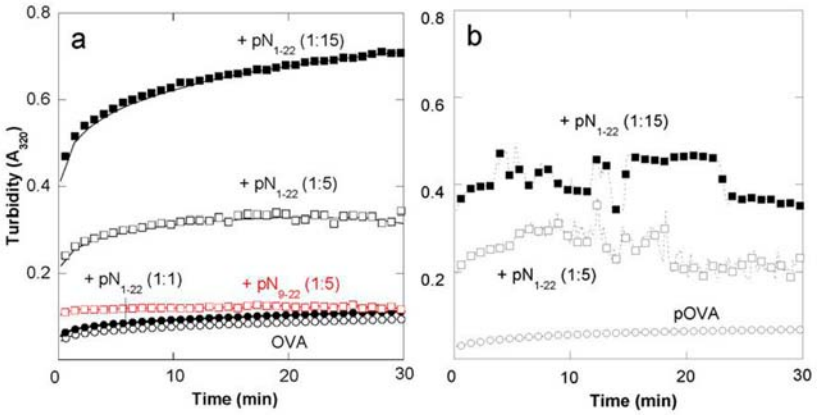

Figure 8. Increase in turbidity with the process of aggregation of OVA (a) and pOVA (b) at 65 °C in the presence of various concentrations of pN_{1-22}. The molar ratio of OVA/peptide is indicated in the figure. The protein solution was diluted in 100 mM phosphate (pH 2.2) preheated to 65 °C. The final protein concentration was 1.0 mg/mL. The red plot is in the presence of pN_{9-22}.

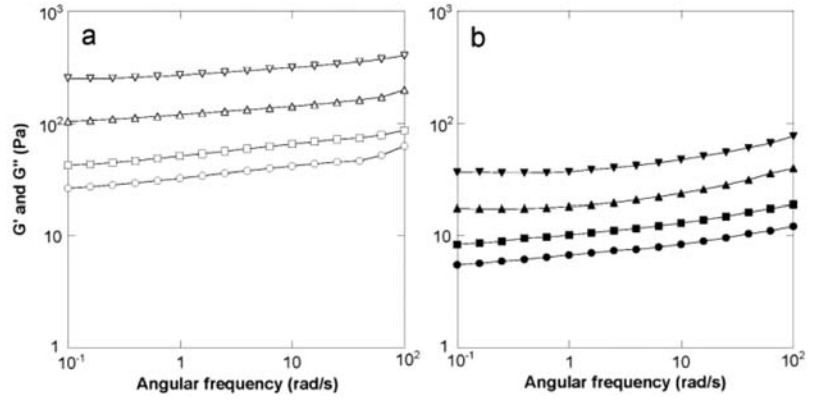

Figure 9. Angular frequency dependence of G' (a) and G'' (b) of the heat-induced OVA gel prepared in the presence of various concentrations of pN_{1-22}: ○ and ●, 2 wt % OVA; □ and ■, +0.3 wt % pN_{1-22} (molar ratio of OVA/peptide = 1:2.7); △ and ▲, +0.6 wt % pN_{1-22} (OVA/peptide = 1:5.4); ▽ and ▼, +1.2 wt % pN_{1-22} (OVA/peptide = 1: 10.8) .

identified as the core region of fibril formation of OVA. Long straight fibrils, which are distinct from the semiflexible fibrillar aggregates of OVA, were formed when OVA was co-incubated with IAIMSA (1:15 molar ratio) at 80 °C under neutral pH conditions. The effect of IAIMSA on OVA aggregation is well explained by its interaction with heat-denatured OVA, which promotes the α-to-β conformational transition. Similarly, pN_{1-22} may bind with heat-denatured OVA to change the morphology of the OVA aggregates to straight fibrils by promoting the α-to-β conformational change of the N-terminal region.

The effect of pN_{1-22} on the morphology of the pOVA aggregates was studied by TEM measurements. When pOVA was co-incubated with pN_{1-22}, straight fibrils that are similar to the fibrils formed in the mixed solution of OVA and pN_{1-22} (Figure S3 in the Supporting Information). The effect of pN_{1-22} on the aggregation of pOVA at pH 2.2 was also studied. The turbidity measurement of pOVA at 65 °C in the presence of pN_{1-22} indicates that the aggregation of pOVA is also accelerated by pN_{1-22} (Figure 8b). However, the turbidity of pOVA aggregates in the presence of pN_{1-22} fluctuated, which is in contrast to the stable turbidity of OVA aggregates in the presence of pN_{1-22}. In a solution of pOVA, the formation of large visible aggregates was detected, and the unstable turbidity may be due to sedimentation of these large aggregates. These results suggest that the effect of pN_{1-22} on the heat-denatured pOVA is similar to that on OVA, but the properties of the pOVA fibrils formed in the presence of pN_{1-22} are distinct from those of OVA fibrils formed in the presence of pN_{1-22}.

The effect of pN_{1-22} on the aggregation of other proteins has been studied by analyzing the heat-induced denaturation of alcohol dehydrogenase (pI = 5.4), firefly luciferase (pI = 6.8), and lysozyme (pI = 11.0) in the presence of pN_{1-22} as reported previously for αA-crystallin.[35] pN_{1-22} promoted the aggregation of these proteins, which have different charges at neutral pH (Supporting Information, Figure S4), suggesting that electrostatic interaction may not be the driving force for protein aggregation. Here, we carried out similar experiments using pN_{9-22} to confirm whether this peptide fragment, which lacks the N-terminal hydrophobic region, has an effect on the aggregation of OVA. As shown in Figure 8a, pN_{9-22} did not significantly promote the heat-induced aggregation of OVA, suggesting that the amphiphilic structure is necessary for the promotion of protein aggregation. Similar papers have suggested that amphiphilic peptides induce soluble proteins to aggregate.[36] Indeed, pN_{1-22} may promote the aggregation of other proteins by acting as a surfactant.

Effect of pN_{1-22} on the Strength of the Protein Gels. We found that the N-terminal amphiphilic region of OVA plays an important role in the aggregation of OVA. Here, we studied the role of the N-terminal amphiphilic region of OVA on the gelation of the protein by analyzing the effect of pN_{1-22} on the

dx.doi.org/10.1021/jf402456v | J. Agric. Food Chem. 2013, 61, 8668−8675

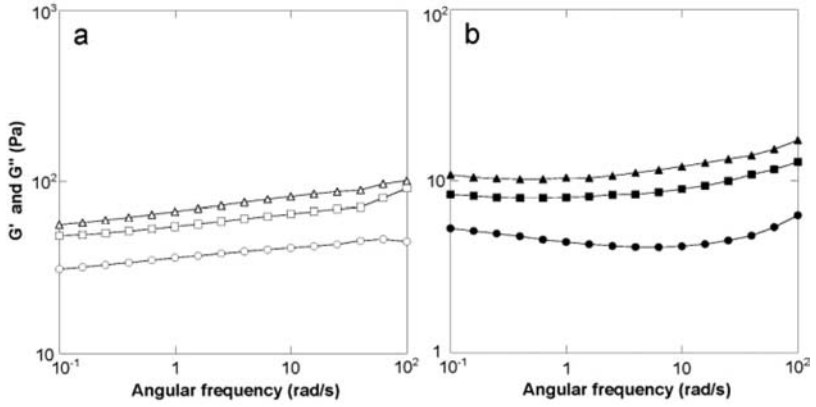

Figure 10. Angular frequency dependence of G' (a) and G'' (b) of the pH-induced gel of collagen I prepared in the presence of various concentrations of pN_{1-22}: ○ and ●, 2.4 mg/mL collagen; □ and ■, + 0.1 mg/mL pN_{1-22} (molar ratio of collagen type I/peptide = 1:6.7); Δ and ▲, + 0.3 mg/mL pN_{1-22} (collagen type I/peptide = 1:20). The molecular mass of the triple helix of collagen I (ca. 400 kDa) was used for the calculation of the molar ratio.

elasticity of the gel. The G' and G'' values of the heat-induced OVA gel prepared in the presence of various concentrations of pN_{1-22} were measured. As shown in Figure 9, the G' and G'' values were increased with increasing concentrations of pN_{1-22} (in the range of 0.3−1.2 wt %). These results clearly show that the N-terminal amphiphilic region of OVA plays an important role in the gelation of OVA by promoting fibril formation. The effect of pN_{1-22} on the gel formation of pOVA was studied under the same conditions. Heat treatment of 2 wt % pOVA in the presence of pN_{1-22} induced the formation of large visible aggregates. Thus, a stable gel for performing reproducible rheological measurements could not be obtained. This may be because the N-terminal amphiphilic region of OVA is necessary for the connected gel network between fibrils, and pOVA fibrils formed in the presence of pN_{1-22} are not sticky enough to form a comprehensive gel-like structure.

To establish whether pN_{1-22} affects the gelation of other proteins, we investigated its effect on the gelation of collagen, one of the most abundant food proteins. Monomeric collagen undergoes self-assembly to generate fiber networks[37] in the form of a gel. A solution of cold type acid-soluble collagen I readily forms a gel when the pH of the solution is neutralized by mixing with reconstitution buffer. To study the effect of pN_{1-22} on elasticity of the collagen I gel, the G' and G'' values of the reconstituted gels were measured. As shown in Figure 10, the G' and G'' values were increased in the presence of pN_{1-22}, indicating that pN_{1-22} increases the gel strength of the collagen I gel. The fiber network of the collagen I gel formed in the absence and presence of pN_{1-22} was monitored by TEM. As shown in Figure 11a, collagen I in the absence of pN_{1-22} forms a well-established network of separated fibrils with a diameter of <10 nm. However, thick and flexible fibrils were formed when collagen I was reconstituted in the presence of pN_{1-22} (Figure 11b). pN_{1-22} may induce the association between triple-stranded collagen molecules and assemble them into the higher ordered fibrils, which would increase the strength of the gel. A detailed study aimed at investigating the molecular mechanism by which pN_{1-22} induces morphological changes in the collagen fibrils is currently underway. Our results indicate that pN_{1-22} could potentially be used as a method for noncovalent cross-linking of collagen gels. Given that pN_{1-22} is a nontoxic peptide derived from food protein, it should be readily applicable to a wide range of uses in the food industry.

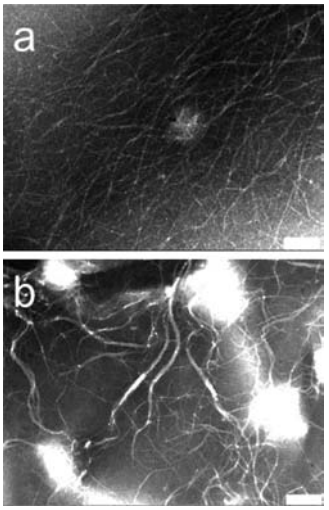

Figure 11. TEM images of fibril of 2.4 mg/mL collagen I reconstituted at neutral pH in the absence (a) and presence (b) of 0.3 mg/mL pN_{1-22}. Scale bar = 200 nm.

In conclusion, we found that the heat-induced aggregation and gelation of pOVA, which lacks the N-terminal amphiphilic region of OVA, are strikingly different from those of OVA. Moreover, pN_{1-22}, a peptide fragment of this amphiphilic region, accelerated the aggregation rate of OVA and induced the formation of straight fibrillar aggregates. pN_{1-22} could bind to the denatured OVA and promote the α-to-β conformational change of the N-terminal region to form straight fibrils. These results support the idea that the N-terminal amphiphilic region plays a significant role in the aggregation process of OVA. The strength of the heat-induced gel of OVA was increased when pN_{1-22} was present during the gelation process. Importantly, the presence of pN_{1-22} during the gelation of collagen was found to increase the strength of the gel. These findings are directly applicable to a wide range of uses in the food industry.

■ ASSOCIATED CONTENT

Ⓢ Supporting Information

Experimental results of the secondary structure of OVA and pOVA monitored by CD spectroscopy, temperature dependence of the partial heat capacity of OVA and pOVA, TEM image of pOVA fibrils formed in the presence of pN_{1-22}, and

effect of pN_{1-22} on the aggregation of ADH, luciferase, and lysozyme. This material is available free of charge via the Internet at http://pubs.acs.org.

AUTHOR INFORMATION

Corresponding Author

*(N.T.) Phone/fax: +81-75-724-7861. E-mail: tanaka@kit.ac.jp.

Notes

The authors declare no competing financial interest.

ACKNOWLEDGMENTS

Tomoko Tada (Kyoto Institute of Technology) is acknowledged for technical assistance.

ABBREVIATIONS USED

OVA, ovalbumin; pOVA, pepsin-treated ovalbumin; pN_{1-22}, peptide fragment of the N-terminal region of ovalbumin composed of residues 1−22

REFERENCES

(1) Stein, P. E.; Leslie, A. G. W.; Finch, J. T.; Turnell, W. G.; McLaughlin, P. J.; Carrell, R. W. Crystal structure of ovalbumin as a model for the reactive centre of serpins. *Nature* **1990**, *347*, 99−102.

(2) Stein, P. E.; Leslie, A. G.; Finch, J. T.; Carrell, R. W. Crystal structure of uncleaved ovalbumin at 1.95 A resolution. *J. Mol. Biol.* **1991**, *221*, 941−959.

(3) Nicolai, T.; Durand, D. Controlled food protein aggregation for new functionality. *Curr. Opin. Colloid Interface Sci.* **2013**, *18*, 249−256.

(4) Tani, F.; Shirai, N.; Onishi, T.; Venelle, F.; Yasumoto, K.; Doi, E. Temperature control for kinetic refolding of heat-denatured ovalbumin. *Protein Sci.* **1997**, *6*, 1491−1502.

(5) Tatsumi, E.; Yoshimatsu, D.; Hirose, M. Conformational state of disulfide-reduced ovalbumin at acidic pH. *Biosci., Biotechnol., Biochem.* **1999**, *63*, 1285−1290.

(6) Tatsumi, E.; Hirose, M. Highly ordered molten globule-like state of ovalbumin at acidic pH: native-like fragmentation by protease and selective modification of Cys367 with dithiodipyridine. *J. Biochem.* **1997**, *122*, 300−308.

(7) Nemoto, N.; Koike, A.; Osaki, K.; Koseki, T.; Doi, E. Dynamic light scattering of aqueous solutions of linear aggregates induced by thermal denaturation of ovalbumin. *Biopolymers* **1993**, *33*, 551−559.

(8) Sagis, L. M.; Veerman, C.; van der Linden, E. Mesoscopic properties of semiflexible amyloid fibrils. *Langmuir* **2004**, *20*, 924−927.

(9) Azakami, H.; Mukai, A.; Kato, A. Role of amyloid type cross β-structure in the formation of soluble aggregate and gel in heat-induced ovalbumin. *J. Agric. Food Chem.* **2005**, *53*, 1254−1257.

(10) Pouzot, M.; Nicolai, T.; Visschers, R. W.; Weijers, M. X-ray and light scattering study of the structure of large protein aggregates at neutral pH. *Food Hydrocolloids* **2005**, *19*, 231−238.

(11) Broersen, K.; Weijers, M.; de Groot, J.; Hamer, R. J.; de Jongh, H. H. Effect of protein charge on the generation of aggregation-prone conformers. *Biomacromolecules* **2007**, *8*, 1648−1656.

(12) Pearce, F. G.; Mackintosh, S. H.; Gerrard, J. A. Formation of amyloid-like fibrils by ovalbumin and related proteins under conditions relevant to food processing. *J. Agric. Food Chem.* **2007**, *55*, 318−322.

(13) Weijers, M.; Broersen, K.; Barneveld, P. A.; Cohen Stuart, M. A.; Hamer, R. J.; De Jongh, H. H.; Visschers, R. W. Net charge affects morphology and visual properties of ovalbumin aggregates. *Biomacromolecules* **2008**, *9*, 3165−3172.

(14) Tanaka, N.; Morimoto, Y.; Noguchi, Y.; Tada, T.; Waku, T.; Kunugi, S.; Morii, T.; Lee, Y. F.; Konno, T.; Takahashi, N. The mechanism of fibril formation of a non-inhibitory serpin ovalbumin revealed by the identification of amyloidogenic core regions. *J. Biol. Chem.* **2011**, *286*, 5884−5894.

(15) Lara, C.; Gourdin-Bertin, S.; Adamcik, J.; Bolisetty, S.; Mezzenga, R. Self-assembly of ovalbumin into amyloid and non-amyloid fibrils. *Biomacromolecules* **2012**, *13*, 4213−4221.

(16) Dobson, C. M. The structural basis of protein folding and its links with human disease. *Nature* **2003**, *426*, 884−890.

(17) Selkoe, D. J. Folding proteins in fatal ways. *Nature* **2003**, *426*, 900−904.

(18) Rousseau, F.; Schymkowitz, J.; Serrano, L. Protein aggregation and amyloidosis: confusion of the kinds? *Curr. Opin. Struct. Biol.* **2006**, *16*, 118−126.

(19) Goto, Y.; Yagi, H.; Yamaguchi, K.; Chatani, E.; Ban, T. Structure, formation and propagation of amyloid fibrils. *Curr. Pharm. Design* **2008**, *14*, 3205−3218.

(20) Sunde, M.; Blake, C. The structure of amyloid fibrils by electron microscopy and X-ray diffraction. *Adv. Protein Chem.* **1997** *50*, 123−159.

(21) Veerman, C.; de Schiffart, G.; Sagis, L. M.; van der Linden, E. Irreversible self-assembly of ovalbumin into fibrils and the resulting network rheology. *Int. J. Biol. Macromol.* **2003**, *33*, 121−127.

(22) Alting, A. C.; Weijers, M.; de Hoog, E. H.; van de Pijpekamp, A. M.; Cohen Stuart, M. A.; Hamer, R. J.; de Kruif, C. G.; Visschers, R. W. Acid-induced cold gelation of globular proteins: effects of protein aggregate characteristics and disulfide bonding on rheological properties. *J. Agric. Food Chem.* **2004**, *52*, 623−631.

(23) Koike, A.; Takada, A.; Nemoto, N. Structure and dynamics of ovalbumin gels: II. Gels induced by heat treatment at 80 °C. *Polym. Gels Networks* **1998**, *6*, 257−271.

(24) Weijers, M.; Sagis, L. M. C.; Veerman, C.; Sperber, B.; van der Linden, E. Rheology and structure of ovalbumin gels at low pH and low ionic strength. *Food Hydrocolloids* **2002**, *16*, 269−276.

(25) Weijers, M.; Visschers, R. W.; Nicolai, T. Light scattering study of heat-induced aggregation and gelation of ovalbumin. *Macromolecules* **2002**, *35*, 4753−4762.

(26) Weijers, M.; Visschers, R. W.; Nicolai, T. Influence of the ionic strength on the structure of heat-set globular protein gels at pH 7. Ovalbumin. *Macromolecules* **2004**, *37*, 8709−8714.

(27) Kitabatake, M.; Doi, E. Heat-induced transparent gels prepared from pepsin-treated ovalbumin and egg white. *Agric. Biol. Chem.* **1985**, *49*, 2457−2548.

(28) Doi, E.; Koseki, T.; Kitabatake, N. Effect of limited proteolysis on functional property of ovalbumin. *J. Am. Oil Chem. Soc.* **1987**, *64*, 1697−1703.

(29) Tani, F.; Shirai, N.; Nakanishi, Y.; Kitabatake, N. Analysis of molecular interaction in heat-induced aggregation of a non-inhibitory serpin ovalbumin using a molecular chaperone. *Biosci., Biotechnol., Biochem.* **2003**, *67*, 1030−1038.

(30) Tabe, L.; Krieg, P.; Strachan, R.; Jackson, D.; Wallis, E.; Colman, A. Segregation of mutant ovalbumins and ovalbumin-globin fusion proteins in *Xenopus* oocytes. Identification of an ovalbumin signal sequence. *J. Mol. Biol.* **1984**, *180*, 645−666.

(31) Arii, Y.; Takahashi, N.; Hirose, M. Periplasmic secretion of native ovalbumin without signal clevage in *Escherichia coli*. *Biosci., Biotechnol., Biochem.* **2003**, *67*, 368−371.

(32) Belin, D.; Guzman, L. M.; Bost, S.; Konakova, M.; Silva, F.; Beckwith, J. Functional activity of eukaryotic signal sequences in *Escherichia coli*: the ovalbumin family of serine protease inhibitors. *J. Mol. Biol.* **2004**, *335*, 437−453.

(33) Weijers, M.; Barneveld, P. A.; Cohen Stuart, M. A.; Visschers, R. W. Heat-induced denaturation and aggregation of ovalbumin at neutral pH described by irreversible first-order kinetics. *Protein Sci.* **2003**, *12*, 2693−2703.

(34) Greenfield, N.; Fasman, G. D. Computed circular dichroism spectra for the evaluation of protein conformation. *Biochemistry* **1969**, *8*, 4108−4116.

(35) Fukuhara, S.; Nishigaki, T.; Miyata, K.; Tsuchiya, N.; Waku, T.; Tanaka, N. Mechanism of the chaperone-like and antichaperone activities of amyloid fibrils of peptides from αA-crystallin. *Biochemistry* **2012**, *51*, 5394−5401.

(36) Zhou, B.; Xing, L.; Wu, W.; Zhang, X. E.; Lin, Z. Small surfactant-like peptides can drive soluble proteins into active aggregates. *Microb. Cell Fact.* **2012**, *11*, 10.
(37) Na, G. C. Monomer and oligomer of type I collagen: molecular properties and fibril assembly. *Biochemistry* **1989**, *28*, 7161−7167.